

A Novel Method of High-Purity Extracellular Vesicle Enrichment from Microliter-scale Human Serum for Proteomic Analysis

Xiaohui Ji^{1,2}, Sisi Huang³, Jie Zhang¹, Terri F. Bruce⁴, Zhijing Tan¹, Donglin Wang², Jianhui Zhu^{1*}, R. Kenneth Marcus^{3*}, and David M. Lubman^{1*}

¹Department of Surgery, University of Michigan Medical Center, Ann Arbor, MI 48109, USA

²Chongqing Key Laboratory of Translational Research for Cancer Metastasis and Individualized Treatment, Chongqing University Cancer Hospital, Chongqing 400030, P. R. China

³Department of Chemistry, Biosystems Research Complex, Clemson University, Clemson, SC 29634, USA

⁴Department of Bioengineering, Life Sciences Facility, Clemson University, Clemson, SC 29634, USA

* Correspondence to: Professor David M. Lubman, Department of Surgery, University of Michigan Medical Center, 1150 West Medical Center Drive, Building MSRB1, Rm A510B, Ann Arbor, MI 48109-0656. Tel: +1-734-647-8834. Fax: +1-734-615-2088. Email: dmlubman@umich.edu; <https://orcid.org/0000-0001-7731-0232>

Dr. Jianhui Zhu, Department of Surgery, University of Michigan Medical Center, 1150 West Medical Center Drive, Building MSRB1, Rm A500, Ann Arbor, MI 48109-0656. Tel: +1-734-615-2567. Fax: +1-734-615-2088. Email: jianhuiz@umich.edu; <https://orcid.org/0000-0002-0051-7777>

Dr. R. Kenneth Marcus, Department of Chemistry, Biosystems Research Complex, Room 106, Biosystems Research Complex, 105 Collings Street, Clemson, SC 29634. Email: marcusr@clemson.edu; <https://orcid.org/0000-0003-4276-5805>

Keywords: Capillary-channeled polymer (C-CP) fibers / Extracellular vesicles / Hydrophobic interaction chromatography (HIC) / Mass spectrometry / Proteomics / Serum

This is the author manuscript accepted for publication and has undergone full peer review but has not been through the copyediting, typesetting, pagination and proofreading process, which may lead to differences between this version and the [Version of Record](#). Please cite this article as [doi: 10.1002/elps.202000223](https://doi.org/10.1002/elps.202000223).

This article is protected by copyright. All rights reserved.

Abbreviations: **BSA**, bovine serum albumin; **C-CP**, capillary-channeled polymer; **CID**, collision-induced dissociation; **DG**, density gradient; **EV**, extracellular vesicle; **FASP**, filter-aided sample preparation; **FDR**, false discovery rate; **HIC**, hydrophobic interaction chromatography; **HPLC**, high-performance liquid chromatography; **ISEV**, International Society for Extracellular Vesicles; **MS**, mass spectrometry; **MWCO**, molecular weight cut-off; **NTA**, nanoparticle tracking analysis; **PBS**, phosphate buffered saline; **PEG**, polyethylene glycol; **PET**, polyethylene terephthalate; **RC**, regenerated cellulose; **RC-CF**, regenerated cellulose centrifugal filter; **SEC**, size exclusion chromatography; **SpCnorm**, normalized spectral counting; **TEM**, transmission electron microscopy; **UC**, ultracentrifugation

Abstract

We have developed a rapid, low-cost, and simple separation strategy to separate extracellular vesicles (EVs) from a small amount of serum (i.e., <100 μ L) with minimal contamination by serum proteins and lipoprotein particles to meet the high purity requirement for EV proteome analysis. EVs were separated by a novel polyester capillary channel polymer (PET C-CP) fiber phase/hydrophobic interaction chromatography (HIC) method which is rapid and can process small size samples. The collected EV fractions were subjected to a post-column cleanup protocol using a centrifugal filter to perform buffer exchange and eliminate potential co-eluting non-EV proteins while minimizing EV sample loss. Downstream characterization demonstrated that our current strategy can separate EVs with the anticipated exosome-like particle size distribution and high yield ($\sim 1 \times 10^{11}$ EV particles per ml of serum) in ~ 15 min. Proteome profiling of the EVs reveals that a group of genuine EV components were identified that have significantly less high-abundance blood proteins and lipoprotein particle contamination in comparison to traditional separation methods. The use of this methodology appears to address the major challenges facing EV separation for proteomics analysis. In addition, the EV post-column cleanup protocol proposed in the current work has the potential to be combined with other separation methods, such as ultracentrifugation (UC), to further purify the separated EV samples.

Additional supporting information may be found in the online version of this article at the publisher's web-site.

Color online: See article online to view Figs. 2–5 in color.

1 Introduction

Extracellular vesicles (EVs) are membrane-enclosed vesicles released to the extracellular space by almost all cells [1,2], which contain RNA, proteins, and DNA derived from their cells of origin [3–5]. Their small size and the ability to penetrate biological barriers make them a unique means of communication between cells via their molecular signatures contained within EVs [6,7]. EVs are potentially an ideal source for biomarkers of early detection and the delivery of therapeutic reagents for disease [8–12]. Due to their diagnostic and therapeutic potential, EVs have become a research focus in the field of medicine in recent years. One of the major topics to be investigated in this field is characterization of EV cargo, including mass spectrometry (MS) based proteomic profiling of their selective protein content for biomarker discovery.

For characterization of the EV protein content for biomarker discovery, it is necessary to separate the EVs from diverse biological fluids. However, it remains challenging to obtain EVs with sufficient purity from complex fluids such as patient serum required for proteomic analysis [13,14]. The most commonly used technologies for EV separation are based on physical properties such as size and density, including ultracentrifugation (UC) [15,16], density gradient (DG) flotation, size exclusion chromatography (SEC) and ultrafiltration. However, a critical issue for these physical separation methods is that they cannot completely separate EVs from lipoproteins and chylomicrons, not only because of the large number of these particles (20- to 100-fold more lipoproteins than EVs), but also because of their physical characteristics (including size and density) which overlap with EVs [17–20]. It has been suggested that > 70% of the particles separated from plasma are non-EVs, which can significantly affect the downstream proteomic analysis [21]. It is also difficult to obtain sufficient purity of EVs from high-abundance blood proteins in serum which interfere with analysis of proteins from EVs by mass spectrometry [17,22]. In addition, the above methods, especially the current gold-standard ultracentrifugation, are more suitable for large sample volumes rather than small volume samples, which could be a disadvantage in both clinical and fundamental applications.

Other EV isolation methods include polymer precipitation [13,23], which relies on the formation of a polymer network to entangle all lipid components in the sample and reduce their solubility for rapid removal at low centrifugal force [24]. Although this method is easy to use, its application is hampered by non-EV protein contaminants and the polymers used to precipitate EVs, e.g., polyethylene glycol (PEG), which can interfere with MS analysis [14,23]. Alternatively, affinity pull-down is superior in selective separation of EVs using specific exosome antibodies, i.e., CD63, CD9, and CD81. However, this separation method may lead to co-elution of antibodies with EVs, and the elution buffer may contain components incompatible with MS[13]. Microfluidic chip-based methods have also been developed to separate EVs from blood samples [25–28]. These separation methods can handle small samples, and the purity of the obtained EVs reaches 98% [26,29]. However, the complicated manufacturing procedure of microfluidic chips and the low throughput of these methods limit their large-scale clinical applications [30].

To obtain higher quality EVs for downstream analysis such as proteomic profiling, there is continuing interest in developing alternative separation methods for high-throughput, high-purity EV enrichment. An alternative approach would be a chemoselective-type of chromatography on a high-performance liquid chromatography (HPLC) platform. The Bruce/Marcus group at Clemson University has recently demonstrated a novel EV separation method using poly (ethylene terephthalate) (PET) capillary-channeled polymer (C-CP) fibers in a hydrophobic interaction chromatography (HIC) protocol. These PET C-CP fiber columns can successfully separate EVs from cell supernatants, urine and plasma, respectively [31–33]. Compared to other traditional technologies, the PET C-CP HIC method is faster (<15 min) and can process small serum samples at the microliter scale, which will be valuable for clinical applications [33,34]. Most recently, the Clemson group has developed a PET C-CP fiber spin-down tip approach that allowed the separation of EVs on a simple table-top centrifuge with high throughput, low cost, and high efficiency [35]. Moreover, this method can effectively separate EVs and lipoprotein particles, which is a critical challenge faced by traditional physical methods for separation of blood EVs. These characteristics make PET C-CP fiber columns a highly promising EV separation method for downstream analysis.

In this study, we have further optimized the PET C-CP HIC method for high-purity EV enrichment from human serum in a small sample amount, i.e., 100 μ L, as well as post-purification processing for characterization and proteomic analysis. This involves 1) the optimization of the elution conditions of the PET C-CP HIC method to increase EV purity, 2) a post-column cleanup step for buffer exchange and further reduction of potential co-purified serum contaminating proteins, and 3) characterization of EVs by multiple techniques and proteomic profiling of EVs. The optimized PET C-CP HIC approach enables effective EV separation serum samples of minimal volume (20 μ L) within a ~15 min chromatographic cycle. The enriched EVs have been characterized by transmission electron microscopy (TEM), nanoparticle tracking analysis (NTA), and Western Blot (WB). We have performed MS-based proteomic analysis of EVs separated by this method to determine the protein categories, EV protein markers, and degree of EV purity. This approach overcomes challenges in EV proteome studies of small volumes of EVs derived from microliter-scale serum. It is believed that this method is promising in both biological studies and practical applications of EVs.

2 Materials and Methods

2.1 Human serum sample

The pooled human serum was purchased from Innovative Research Inc. (Novi, MI). Each donor unit was tested and found negative for HBsAG, HIV-1/2, anti-HCV, anti-HBs, anti-HBc, HCV-NAT, HIV-1 NAT in conformance with FDA regulations. The pooled serum was filtered through a 200 nm cartridge. After purchase, it was aliquoted and stored at -80°C until further use to avoid freeze-thaw cycles.

2.2 EV separation by HIC method with a PET C-CP fiber column

All chromatographic measurements were performed on a Dionex Ultimate 3000 HPLC system (LPG-3400SD quaternary pump and MWD-3000 UV–Vis absorbance detector; Thermo Fisher Scientific, Sunnyvale, CA) and controlled by the Chromeleon 7 software system as reported previously [32]. Detection at 216 nm was used. Isolated fractions from the HPLC were collected using an R1 fraction collector (Teledyne Isco, Lincoln, NE).

The in-house PET C-CP fiber column has been described in our previous study [36]. The HIC method previously developed for the isolation of exosomes from human blood plasma [33] was employed here with minor modifications. In brief, the PET C-CP fiber column was equilibrated with 2 M $(\text{NH}_4)_2\text{SO}_4$ (VWR, Sokon, OH) dissolved in PBS, pH = 7.4, which also serves as the loading medium. The separation was performed at a flow rate of 0.5 mL/min. In each separation cycle, 20 μL of serum was directly loaded onto the PET C-CP fiber column. After washing the column with the loading medium for 2 min, two gradient steps were employed sequentially, i) 25% glycerol (VWR, Sokon, OH) with 1M $(\text{NH}_4)_2\text{SO}_4$ to remove blood proteins and ii) 50% glycerol in PBS to elute the bound EVs from the column. To optimize the method and reduce blood protein components in the EV fraction, the first gradient step was performed for different time windows (4, 6, 8, 10, and 12 min, respectively).

2.3 Development of a post-column cleanup protocol

Three Amicon Ultra-4 regenerated cellulose (RC) centrifugal filters (MWCO 10/50/100 kDa) (Millipore Sigma, St. Louis, MO) were tested to establish a post-column cleanup protocol for the collected EV fraction. The purpose of the protocol is a buffer exchange into PBS (preferable for MS analysis) and to eliminate the minimal co-eluted blood proteins while minimizing sample loss of EVs. The protocol was first tested on an EV standard (ab239690, Abcam, Cambridge, MA). Aliquots of 10 μg EV standard were diluted with 4 mL PBS and then centrifuged on the three different MWCO filters at 3,700 g and 4°C. With the final volume of 100 μL , the sample was concentrated about 40-fold. The concentrated samples were retrieved by pipetting. The filter membrane was then rinsed with 100 μL PBS and the liquid was then combined with the concentrate. Proteins adsorbed onto the Amicon Ultra-4 RC 100kDa centrifugal filter were recovered by repetitive washing of the membrane with 200 μL 0.4% SDS [37]. The EV samples for MS-based proteomic analysis were dried down immediately using a SpeedVac (Labconco, Kansas City, MO) after cleanup. The EV samples for NTA and TEM analysis were directly analyzed after cleanup treatment without need for freezing.

2.4 Nanoparticle tracking analysis (NTA)

The recoveries of commercial “standard” EVs by the above three centrifugal filters and the separated serum-derived EVs were evaluated using the NanoSight NS300 (Malvern, Worcestershire, U.K.). Each EV sample was diluted using 200 nm-filtered PBS to the optimal concentration range of the NTA Software and continuously infused into the NanoSight by an

automatic syringe pump at a flow rate of 25 $\mu\text{L}/\text{min}$. The focus was adjusted and the dilution factor was set according to the dilution of the sample. For each sample, particles moving under Brownian motion were recorded on video five times, for 30s each. The concentration of EVs was then calculated by the NTA software (v3.3).

2.5 Transmission Electron Microscopy (TEM)

TEM was used to measure the size and morphology of the EVs. First, glow discharge processing was performed to make the surface of the carbon film (Hatfield, PA) hydrophilic. The separated EV sample was diluted by PBS, where 5 μL was dropped on the carbon film and incubated for 2 min. Next, 5 μL of 2.5% w/v glutaraldehyde was used to fix the EVs for 5 min. The film was negatively stained using 5 μL of 1% uranyl acetate for 1 min. After each of the above steps, the liquid was removed by a small piece of filter paper. EVs on carbon films were then imaged using a JEOL 1400-plus transmission electron microscope.

2.6 1D SDS-PAGE and Western Blot

SDS-PAGE analysis of the EV proteins was performed by SDS-PAGE gel (Bio-Rad, Berkeley, CA) followed with silver staining using a ProteoSilver Plus Silver Stain Kit (Sigma). For EV fractions with different elution times, 6 min and 14 min, respectively, the EV proteins derived from 40 μL of serum were loaded onto the gel, with 0.05 μg of BSA standard protein (Abcam, Cambridge, MA) employed as a reference. For the concentrates filtered by the three Amicon RC centrifugal filters (MWCO 10/50/100 kDa), the EV proteins from the same amount of 10 μg of EV standard were loaded onto the gel, with BSA again employed as a reference.

EV proteins ($\sim 5 \mu\text{g}$) were separated by SDS-PAGE gel (Bio-Rad, Berkeley, CA) and transferred to a PVDF membrane (Bio-Rad, Berkeley, CA). The PVDF membranes were blocked for 1h at room temperature in PBST containing 5% milk and incubated overnight at 4°C with the following primary antibodies in PBST containing 2% BSA: mouse anti-human CD9 monoclonal antibody (1:1000) (ab254175, Abcam, Cambridge, UK) and mouse anti-human CD63 monoclonal antibody (1:1000) (ab1318, Abcam, Cambridge, UK). After incubation with appropriate HRP-conjugated secondary antibodies (1:3000) in PBST containing 2.5% milk, blots were performed using Super signal Chemiluminescence Reagent (Thermo Scientific, Rockford, IL).

2.7 Mass spectrometry and bioinformatics analysis

After collecting the concentrate from the Amicon Ultra-4 centrifugal filter, 200 μ L of 0.4% SDS solution was used to wash the inner surface of the filter to recover the EVs (to be more precise, EV proteins) adhered to the filter surface. The concentrated sample was dried immediately using a SpeedVac (Labconco, Kansas City, MO), after which EV proteins were extracted and digested according to the filter aided sample preparation (FASP) procedure as previously reported [38].

The tryptic digests of the sample were desalted by homemade C18 tips [39] and then on a Dionex UHPLC system (Thermo Fisher Scientific, San Jose, CA) with a 250 mm reverse-phase (RP) C18 column. The samples were resolved under a 120 min linear gradient from 2 to 35% acetonitrile in 0.1% formic acid at a constant flow rate of 300 nL/min. The samples were analyzed on an Orbitrap Lumos mass spectrometer (Thermo Fisher Scientific), operated in the positive ion mode. The capillary temperature and the spray voltage were set at 200°C and 1.7 kV, respectively. The data were acquired in a data-dependent mode, where up to 20 of the strongest intensity primary MS peaks were selected for subsequent MS2 analysis. Every selected peak, collision-induced dissociation (CID) was performed. The normalized collision energy was set at 34% for MS/MS. The broadband spectra (m/z 350–1650) and the MS2 spectra were acquired in the Orbitrap and linear ion trap, respectively.

All raw data files were processed by the Proteome Discover platform (version 1.6.1.0) [40]. The parameters were set as follows: database, human UniProt; enzyme, trypsin; fixed modification, carbamidomethyl (C); variable modifications, oxidation (M); up to two missed cleavages allowed. The MS mass tolerance was set as 10 ppm; the MS2 mass tolerance was set as 0.5 Da. The false discovery rates (FDRs) for peptides and proteins were both set as 1%. Gene ontology analysis of all identified proteins was investigated with FunRich V3.1.3 using the Gene Ontology Database [41,42]. The Vesiclepedia database search was also performed in the FunRich software environment [41,43].

2.8 EV marker list

We investigated the MS results for the markers of EVs recommended by the International Society for Extracellular Vesicles (ISEV) in the "Minimal information for studies of extracellular vesicles 2018 (MISEV2018): a position statement of the International Society for Extracellular Vesicles and update of the MISEV2014 guidelines" [44] (Supporting Information Table S1).

2.9 Label-free spectral counting for relative quantitation of the top 10 serum proteins and major apolipoproteins

Proteins identified from EV samples were quantified using a label-free quantitative method termed the normalized spectral counting (SpCnorm) [45,46]. In brief, the spectral count of each individual protein was normalized against the sum of the spectral counts of all proteins

identified in an MS run. We investigated two groups of contaminating proteins, the top 10 serum proteins and major apolipoproteins, respectively, in the EV samples. Ten of the most abundant proteins represent 90% of the total serum protein mass [47,48]. Lipoprotein particles are very abundant in the blood, with a diameter of 25–1200nm while apolipoprotein is one of the main components of lipoprotein particles, including apolipoprotein A/B/C/E [18]. The list of 27 representative major serum contaminating proteins is summarized in Supporting Information Table S2. The relative abundance of proteins in the two protein groups was summed respectively to represent the percentage content of the top 10 serum proteins and apolipoproteins detected in the EV sample.

2.10 Statistical analysis

Data analysis and graphical presentations were performed using GraphPad Prism 8 (Graphpad Software, San Diego, CA). An unpaired Student's t-test was applied for determination of significant difference in recovery of EVs between the three Amicon Ultra-4 centrifugal filters. P values of less than 0.05 indicated statistical significance. Data are expressed as mean \pm SD.

3 Results and discussion

3.1 EV separation by an optimized PET C-CP fiber HIC method

In our previous studies, the step gradient HIC method coupled with a PET C-CP column was used for EV separation from different matrices and showed the isolation of the target EV from proteins in human urine and plasma samples [31–33]. In that method, salts and small molecules were eluted during the loading step (2 min), proteins and other macromolecules eluted at the first gradient step, and the lone-remaining EVs were eluted at the second gradient step. Serum is a very difficult substrate for EV proteomic study as the presence of high-abundance serum proteins and non-EV lipid particles hampers the ability to detect low-abundance EV-related proteins by untargeted shotgun mass spectrometry approaches. Our previous studies have fully confirmed that this method can successfully separate EVs from a variety of matrices with a high recovery. However, MS-based proteomics analysis has high requirements for sample purity. When the EV samples separated by this method were used for MS-based proteomics analysis, we found that it was still subject to a certain degree of serum high-abundance protein contaminants.

Thus, to obtain higher purity EV samples meeting the requirements of MS-based proteomic analysis, we further optimized the PET C-CP HIC method and added a post-column buffer exchange/polishing protocol with different RC centrifugal filters for down-stream EV characterization and EV proteome profiling, respectively. The workflow is summarized in Figure 1.

For the PET C-CP HIC method, we extended the first gradient step up to 12 min to optimize the elution time of the high-abundance proteins characteristic of serum media. Figure 2A shows the representative chromatograms of human serum samples with UV-Vis detector responses at 216 nm by varying the hold-time of the first gradient step (4, 6, 8, 10, and 12 min respectively). The peak corresponding to the elution of EVs was delayed accordingly with the increased hold-time of the first gradient where the second gradient steps were initiated at 6, 8, 10, 12, and 14 min, respectively. For example, the black line shows the chromatogram with a 4-min long first gradient step (i.e., EV elution step time of 6 min). There is an injection peak in each chromatogram, corresponding to non-retained species such as salts and small polar molecules during the loading step (0–2 min). The intense and broad peak between 2 and 6 min reflects the elution of proteins during the first gradient step and EVs were then eluted afterwards with the second gradient step. The extension of the hold-time of the first gradient step resulted in a decrease in the apparent recovery of the EVs in the second gradient step. As shown in the table, the peak areas for the second gradient step decreased gradually as a function of the hold-time, appearing to approach a stable level as the second step initiation time exceeded 12 min. The decrease in absorbance observed here is interpreted as a higher purity of EVs eluting as blood proteins were removed to a greater extent at the longer first gradient hold-times. This hypothesis was further confirmed by SDS-PAGE (Silver staining) analysis of the eluted EVs from 40 μ L of serum. Here we chose albumin as being representative of high-abundance serum contaminating proteins. As shown in Figure 2B, in comparison to the second step initiation time of 6 min, the gradient step initiated at 14 min yields a significantly-reduced albumin band, indicating that extending the hold-time of the first gradient does indeed provide higher-purity EV fractions.

3.2 Establishment of a post-column cleanup protocol for concentration and further purification of collected EV fractions

The EV fraction was collected in elution buffer containing 50% glycerol. Therefore, a post-column cleanup protocol using a centrifugal filter was developed for sample concentration, buffer exchange and further reduction of potentially co-eluting free serum contaminating proteins prior to downstream proteomic analyses. In EV separation protocols, centrifugal filters have been commonly used for sample concentration or buffer exchange. They are available with different membrane types and multiple pore sizes. It has been reported that centrifugal filters formed from regenerated cellulose (RC) membranes have higher recoveries than other membrane types due to the weak EV binding capacity [37]. Herein, we compared the efficiency of three RC centrifugal filters with different pore sizes, including the Amicon 10kDa RC, 50kDa RC, and 100kDa RC, in concentrating a defined number of commercial standard EVs in PBS.

For each filter, a 4 mL sample (10 μ g EVs in PBS) was concentrated 40-fold (final volume of 100 μ L) by centrifugation at 3,700 g for 3 cycles at 4°C. The original and the concentrated EV samples were analyzed by NTA to evaluate the recovery of the EVs. A comparative analysis of the recovery rate ([particle concentration after centrifugation/particle

concentration before centrifugation] $\times 100\%$) of the three filters is shown in Figure 3A, where the Amicon 10kDa RC generates the highest EVs recovery (mean = 87.13%). The EV recovery of the Amicon 50kDa RC and 100kDa RC filters was significantly lower as compared to the Amicon 10kDa RC ($p = 0.0028$ and 0.0005 respectively).

The trend of decreasing in EV recovery was consistent with previous reports [34]. Vergauwen et al. reported that the EV recovery of Amicon 10kDa RC and 100kDa RC filters were $\sim 100\%$ and $\sim 40\%$ [37], respectively, but no data of the Amicon 50kDa RC filter was discussed in their study. Although the recovery rates obtained by the two studies are slightly different, which may be due to different centrifugation settings (speed, time, etc.) and sample volumes, both studies showed that the 10kDa RC filter can recover most of the EVs, while the 100kDa RC filter results in a large amount of EV loss. The pore sizes of the Amicon 10kDa/50kDa/100kDa RC filters (~ 2.5 nm, ~ 5 nm, and ~ 10 nm, respectively) are much smaller than the diameter of the EVs, and NTA measurements of the filtrates showed that almost no particles were observed, so the loss of EVs through the membrane pores can be ruled out. However, the EVs were more likely adsorbed to the membrane pores of the 50kDa/100kDa filters as compared to the 10kDa filter, showing a correlation between the affinity effect and the pore size of the filter membrane. Other research has also verified that the EVs were attached to the inner surface of the filter rather than passing through the filter [37].

To fully evaluate the efficiency of the above three filters in removing potential contaminating proteins in EV fractions, SDS-PAGE of the concentrates were carried out followed by silver staining. As shown in Figure 3B, as the MWCO of the filter membrane increased, the protein content of the concentrate decreased significantly. Based on the results of the EV recovery above, this is mainly due to the loss of EVs caused by adhesion to the inner membrane surface of the filter. The standard EVs we used were separated from the culture medium, and bovine serum albumin (BSA, MW = 66.5 kDa) was one of the main contaminating proteins. From the SDS-PAGE result in Figure 3B, with $0.05 \mu\text{g}$ of BSA standard protein as a reference, it can be seen that the BSA protein band was dramatically decreased in the concentrate of the 50kDa RC filter and was absent in the concentrate of the 100kDa filter. With sample concentration and buffer exchange by centrifugal filters, we realized another opportunity to further purify the sample. Each RC centrifugal filter, with a defined MWCO, represents their ability to retain molecules above a specified molecular weight. During the centrifugation, proteins with a molecular weight less than the MWCO value of the filter, especially those less than 2 times, are likely filtered out and removed.

The results indicate that the choice of centrifugal filter may critically impact the recovery of EVs during the post-column procedure. For our current research, as shown above, although Amicon 10kDa RC achieved the highest recovery of EVs, it could not effectively filter out the residual co-purified free contaminating proteins. In contrast, Amicon 100kDa RC can effectively remove the free contaminating proteins with relatively low MW (Particularly $< 50\text{kDa}$), but it resulted in a significant loss of EVs as compared to the Amicon 10kDa RC. Our aim is to establish a post-column cleanup protocol not just for sample concentration and buffer exchange, but also for further purification of the collected EV fractions. Based on the

downstream analysis requirements and taking advantage of both Amicon 10kDa RC and Amicon 100kDa RC, our post-column cleanup protocol was developed as: 1) downstream NTA / TEM / WB analysis, a 10kDa RC filter for sample concentration; 2) MS-based proteomics analysis, a 100kDa RC filter for sample concentration and further purification followed by a 0.4% SDS solution to wash the inner surface of the filter to recover the EVs (EV proteins) adsorbed to the filter surface [37].

3.3 EV characterization

After establishing the cleanup protocol, we applied it to the collected serum sample EV fractions. According to the protocol, for EV characterization analysis (NTA/TEM/WB), the eluted EV fractions were buffer exchanged into PBS by the Amicon Ultra-4 10kDa RC centrifugal filter and concentrated to about 100 μ L.

As shown in the TEM images (Figure 4A), the separated EVs were \sim 30–150 nm in diameter, and an intact vesicle structure and typical cup-shaped morphology was found, indicating that the lipid bilayer is retained during the PET C-CP fiber HIC separation. The TEM images also displayed a relatively clear background. As revealed by NTA measurement in Figure 4B, the size distribution of the EVs isolated using the PET C-CP fiber HIC method peaks at an average size of 90–120nm and there are two lower-concentration fractions of the particles around 35 nm and 200 nm, reflecting an exosome-like particle diameter distribution. The number of EVs isolated from 0.1 mL of serum by the PET C-CP fiber HIC method was $\sim 1 \times 10^{10}$, or equivalent to number of $\sim 1 \times 10^{11}$ from 1 mL of serum.

Our laboratory has previously used UC and SEC methods to separate EVs from serum, with the results showing that these two methods can recover $\sim 1.5 \times 10^9$ and $\sim 1.3 \times 10^9$ particles, respectively, from 1 ml of serum [49]. Therefore, the current PET C-CP fiber HIC method achieved an $\sim 10^2$ higher yield than the UC and SEC methods. Moreover, the Clemson group's most recent research has demonstrated that this method can effectively separate EVs and lipoprotein particles, which is a critical challenge faced by traditional physical methods (based on density or size) for separation of blood EVs. Several studies have confirmed that a large fraction of the "EVs" obtained by separation methods based on particle density or size are actually lipoprotein and chylomicron particles [17,19–21]. As a final point, two common exosome markers, CD63 and CD9, were evaluated for the EV fractions by Western blot. As shown in Figure 4C, CD63 and CD9 were observed in the Western blot results of EVs extracted from serum by the PET C-CP fiber HIC method, which further confirmed that the vesicles separated were EVs.

3.4 Proteomic analysis reveals that the EVs separated using our current strategy are devoid of highly abundant serum proteins and lipoprotein particles

After demonstrating the high recovery of EVs (with a size range reflective of exosomes) of the PET C-CP HIC separation method combined with the polishing protocol, MS-based proteomic analysis was performed to examine the proteomic profile of separated EVs. In total, 496 proteins were identified from 100 μ L serum samples in three replicates (after removal of keratins), and 56.5% of the proteins could be identified in at least two of the three replicates (Supporting Information Table S3). A total of 80 proteins were identified from the top 100 human EV proteins listed on Vesiclepedia database, as well as some of the EV markers recommended by MISEV2018 [44] such as CD63, CD81 and CD82 (Table 1). As shown in Figure 5A, most of the proteins identified have been previously reported by Vesiclepedia. Gene ontology analysis of cell components of the identified proteins shows that exosomes were the most enriched item (73.7%), followed by cytoplasm (58.9%) and plasma membrane (44%), supporting the conclusion that the group of EV-derived proteins are highly enriched by the current separation strategy (Figure 5B). Prevalent molecular functions of identified proteins were assigned as neutrophil degranulation (16.9%), negative regulation of apoptotic process (8.1%) and Post-translational protein modification (7.2%) (Figure 5C). Identified proteins were confidently assigned ($p < 0.001$) to three molecular functions: identical protein binding (85.7%), RNA binding (22.2%) and Cadherin binding (19%) (Figure 5D).

The quantitative dynamic range of serum proteins is estimated to span 10–12 orders of magnitude where only 10 high abundance proteins constitute 90% of the total proteins [47,48]. In fact, only 1% of the entire protein content of serum as well as EV protein content consists of low abundance proteins, which are of greatest interest in proteomic studies in search of potential biomarkers [48]. Besides high abundance serum proteins, the number of lipoprotein particles in serum far exceeds that of EVs, and their physical properties such as size and density also partially overlap with EVs [17,18,20]. These characteristics explain why it is such a difficult task to separate EVs from serum/plasma to meet the purity requirements of MS-based proteomics analysis, especially when dealing with small sample volumes.

To evaluate the effectiveness of our current strategy to enrich EV proteins, which involves the ability to deplete high-abundance serum proteins and lipoprotein particles, semi-quantitative normalized spectral counting was carried out to determine the relative abundance of the top 10 serum proteins and apolipoproteins within the sample. We compared the percentage content of the contaminating proteins in the serum-derived EV samples between this study and our previous study that used three different separation methods, optimized UC, SEC (qEV) and UC&SEC (qEV) [49] (Supporting Information Table S4). As shown in Figure 6A, the average percentage content of the top 10 serum proteins in the EV samples separated by the PET C-CP fiber HIC method, UC, SEC (qEV) and UC&SEC (qEV) was 12.69%, 25.19%, 19.60%, and 21.17%, respectively, while the average percentage content of apolipoproteins was 3.65%, 5.47%, 38.23% and 19.32%, respectively. These results demonstrate that our current separation strategy can significantly reduce the contamination of high-abundance serum proteins (such as albumin and globulin) as well as problematic lipoprotein particles.

Our results indicate that apolipoproteins (representing lipoprotein particles), which is one of the biggest challenges currently encountered by EV separation methods, are significantly removed from the EVs by the PET C-CP HIC method. It thus confirms that the PET C-CP HIC method can effectively separate EVs and lipoprotein particles. This excellent performance may be attributed to the PET C-CP HIC method based on hydrophobic interaction chromatography rather than the physical properties such as size and density. For example, the surface of LDL particle is surrounded by a single-layer, hydrophilic membrane consisting of phospholipids, free cholesterol, and apolipoproteins [18], while the outer membrane of an EV is a phospholipid bilayer that is more hydrophobic in nature [50].

To further evaluate the purity of EV samples obtained by our current separation strategy, we also compared our data with several other studies. As shown in Figure 6B, the average percentage content of the top 10 serum proteins and apolipoproteins in EV samples obtained by UC in the study of Y. Chen et al. were 34.63% and 3.66%, respectively [51] (Supporting Information Table S5). The average percentage contents of those serum proteins and apolipoproteins in EV samples in the study of A. de Menezes-Neto et al. were 24.43% and 26.41%, respectively, for the SEC (Sepharose CL-2B) method and 50.12% and 8.64%, respectively for the precipitation (Exo-spin) method [22] (Supporting Information Table S6). The results indicate that, as compared with several currently used separation methods, the PET C-CP HIC method yields higher purity EVs with minimal contamination from serum proteins and apolipoproteins.

Ultracentrifugation (UC) is the current gold-standard of commonly-used isolation method for EVs. Our results show that in comparison to the SEC or precipitation, EVs separated by the UC are indeed of higher purity. However, there is still a large amount of high-abundance protein contamination (34.63%) [51] associated with the EV sample, which is consistent with the results reported by many previous studies. Our laboratory has optimized the UC method [15,49], that is, the EV pellet obtained by the first UC is subjected to another 4 cycles of UC and washing. In comparison to one cycle of UC, the optimized UC method can reduce serum high-abundance protein contamination (25.19% vs. 34.63%). However, when compared to the present PET C-CP HIC method, the content of high-abundance serum contaminating proteins and apolipoproteins in EVs separated by the optimized UC method was still higher.

At present, SEC and precipitation are two other commonly used separation methods for EVs. Our results show that when SEC or precipitation was used alone, the isolated EVs contain a large amount of contaminating proteins, which is consistent with the results of many previous studies [17,22,23,49]. In addition, we found that, contrary to the UC method, the main contaminant of EVs separated by the SEC was apolipoproteins (qEV 38.23%, Sepharose CL-2B 26.41%), not serum high-abundance soluble proteins (qEV 19.60%, Sepharose CL-2B 24.43%). Brennan et al. used Western Blot to also prove that when compared with UC or precipitation (ExoQuick plus), the samples of EVs separated using SEC had the highest apolipoproteins content [52]. This may be attributed to the fact that the size of lipoprotein particles is close to or partially overlaps with that of EV particles, which results in SEC (based on particle size) having a poorer resolution for lipoprotein particles. Among all of the separation methods analyzed above, the samples separated by precipitation (Exo-spin) had

the highest content of contaminating proteins. However, unlike SEC, the main contaminating protein of EVs separated by precipitation (Exo-spin) was soluble serum high-abundance proteins. These results indicate that, in comparison to the PET C-CP HIC method, SEC or precipitation alone have obvious limitations in profiling the EV proteome due to the contamination of high-abundance serum proteins or lipoprotein particles.

4 Concluding remarks

In summary, the optimized PET C-CP HIC separation strategy coupled with a post-column cleanup protocol shows improved EV enrichment with a comparable yield of $\sim 1 \times 10^{10}$ EVs from 100 μL of serum in ~ 15 min and can significantly reduce the contamination of non-EV proteins, especially lipoprotein particles, in comparison to the currently available EV separation methods. This EV separation platform shows the advantage in small sample volume (< 100 μL of serum), reduced laboratory work, high EV recoveries, and low contamination, which make it possible to include EV biomarker evaluation in routine blood tests for monitoring disease progression and/or therapeutic response during a course of treatment. The comparison of RC centrifugal filters with three different pore sizes (MWCO 10kDa/50kDa/100kDa) reveals that the 10kDa RC filter has the highest EV recovery while the 100kDa RC filter maximally eliminates co-eluting serum protein contaminants, which can be combined with other EV separation methods. The optimized PET C-CP HIC method provides a useful means of separating sufficient numbers of EVs while meeting the purity requirements of MS-based proteomic analysis from microliter-scale serum samples. While the method employed here involves the use of a standard laboratory HPLC system, the recently-described use of a spin-down mode of HIC processing on C-CP fiber tips using a benchtop centrifuge may ultimately be the preferred mode of microliter sample volume processing [35].

Acknowledgement

This work was supported by the National Institutes of Health under grant R01GM49500 (D.M.L.) and the National Cancer Institute under grants R21CA189775 (D.M.L.) and R50 CA221808 (J.Z.), and partially supported under grant R01 CA160254 (D.M.L.). D.M.L. acknowledges support under the Maud T. Lane Professorship. PET C-CP HIC method and materials development work at Clemson University was supported by the National Science Foundation, Division of Chemistry under grant CHE-1608663. Financial support for the exosome isolation efforts from the Eppley Foundation for Scientific Research is gratefully acknowledged. The Gibson Foundation and the Prisma Health System (Greenville, SC) are gratefully acknowledged.

Conflict of interest:

The authors have declared no conflict of interest.

5 References

- [1] Yanez-Mo, M., Siljander, P. R., Andreu, Z., Zavec, A. B., Borrás, F. E., Buzas, E. I., Buzas, K., Casal, E., Cappello, F., Carvalho, J., Colas, E., Cordeiro-da Silva, A., Fais, S., Falcon-Perez, J. M., Ghobrial, I. M., Giebel, B., Gimona, M., Graner, M., Gursel, I., Gursel, M., Heegaard, N. H., Hendrix, A., Kierulf, P., Kokubun, K., Kosanovic, M., Kralj-Iglic, V., Kramer-Albers, E. M., Laitinen, S., Lasser, C., Lener, T., Ligeti, E., Line, A., Lipps, G., Llorente, A., Lotvall, J., Mancek-Keber, M., Marcilla, A., Mittelbrunn, M., Nazarenko, I., Nolte-'t Hoen, E. N., Nyman, T. A., O'Driscoll, L., Oliván, M., Oliveira, C., Pallinger, E., Del Portillo, H. A., Reventos, J., Rigau, M., Rohde, E., Sammar, M., Sanchez-Madrid, F., Santarem, N., Schallmoser, K., Ostefeld, M. S., Stoorvogel, W., Stukelj, R., Van der Grein, S. G., Vasconcelos, M. H., Wauben, M. H., De Wever, O., *J. Extracell. Vesicles* 2015, 4, 27066.
- [2] Lasser, C., *Expert Opin. Biol. Ther.* 2015, 15, 103–117.
- [3] Valadi, H., Ekstrom, K., Bossios, A., Sjostrand, M., Lee, J. J., Lotvall, J. O., *Nat. Cell Biol.* 2007, 9, 654–659.
- [4] Raposo, G., Stoorvogel, W., *J. Cell Biol.* 2013, 200, 373–383.
- [5] Lazaro-Ibanez, E., Sanz-Garcia, A., Visakorpi, T., Escobedo-Lucea, C., Siljander, P., Ayuso-Sacido, A., Yliperttula, M., *Prostate* 2014, 74, 1379–1390.
- [6] Zhang, J., Li, S., Li, L., Li, M., Guo, C., Yao, J., Mi, S., *Genomics Proteomics Bioinformatics* 2015, 13, 17–24.
- [7] Chen, I. H., Xue, L., Hsu, C. C., Paez, J. S., Pan, L., Andaluz, H., Wendt, M. K., Iliuk, A. B., Zhu, J. K., Tao, W. A., *Proc. Natl. Acad. Sci. U. S. A.* 2017, 114, 3175–3180.
- [8] Melo, S. A., Luecke, L. B., Kahlert, C., Fernandez, A. F., Gammon, S. T., Kaye, J., LeBleu, V. S., Mittendorf, E. A., Weitz, J., Rahbari, N., Reissfelder, C., Pilarsky, C., Fraga, M. F., Piwnicka-Worms, D., Kalluri, R., *Nature* 2015, 523, 177–182.
- [9] Zhang, W., Xia, W., Lv, Z., Ni, C., Xin, Y., Yang, L., *Cell Physiol. Biochem.* 2017, 41, 755–768.
- [10] Khan, M., Nickoloff, E., Abramova, T., Johnson, J., Verma, S. K., Krishnamurthy, P., Mackie, A. R., Vaughan, E., Garikipati, V. N., Benedict, C., Ramirez, V., Lambers, E., Ito, A., Gao, E., Misener, S., Luongo, T., Elrod, J., Qin, G., Houser, S. R., Koch, W. J., Kishore, R., *Circ. Res.* 2015, 117, 52–64.
- [11] Arbeláiz, A., Azkargorta, M., Krawczyk, M., Santos-Laso, A., Lapitz, A., Perugorria, M. J., Erice, O., Gonzalez, E., Jimenez-Aguero, R., Lacasta, A., Ibarra, C., Sanchez-Campos, A., Jimeno, J. P., Lammert, F., Milkiewicz, P., Marzioni, M., Macias, R. I. R., Marin, J. J. G., Patel, T., Gores, G. J., Martinez, I., Elortza, F., Falcon-Perez, J. M., Bujanda, L., Banales, J. M., *Hepatology* 2017, 66, 1125–1143.
- [12] Wang, N., Song, X., Liu, L., Niu, L., Wang, X., Song, X., Xie, L., *Cancer Sci.* 2018, 109, 1701–1709.
- [13] Abramowicz, A., Widlak, P., Pietrowska, M., *Mol. Biosyst.* 2016, 12, 1407–1419.
- [14] Keller, B. O., Sui, J., Young, A. B., Whittall, R. M., *Anal. Chim. Acta* 2008, 627, 71–81.
- [15] An, M., Lohse, I., Tan, Z., Zhu, J., Wu, J., Kurapati, H., Morgan, M. A., Lawrence, T. S., Cuneo, K. C., Lubman, D. M., *J. Proteome Res.* 2017, 16, 1763–1772.

- [16] Kim, J., Tan, Z., Lubman, D. M., *Electrophoresis* 2015, 36, 2017–2026.
- [17] Karimi, N., Cyjetkovic, A., Jang, S. C., Crescitelli, R., Hosseinpour Feizi, M. A., Nieuwland, R., Lotvall, J., Lasser, C., *Cell. Mol. Life Sci.* 2018, 75, 2873–2886.
- [18] Feingold, K. R., Grunfeld, C., *Introduction to Lipids and Lipoproteins*, in: Feingold, K. R., Anawalt, B., Boyce, A., Chrousos, G., Dungan, K., Grossman, A., Hershman, J. M., Kaltsas, G., Koch, C., Kopp, P., Korbonits, M., McLachlan, R., Morley, J. E., New, M., Perreault, L., Purnell, J., Rebar, R., Singer, F., Trencze, D. L., Vinik, A., Wilson, D. P. (Eds.), *Endotext*, MDText.com, Inc., South Dartmouth (MA) 2000.
- [19] Yuana, Y., Levels, J., Grootemaat, A., Sturk, A., Nieuwland, R., *J. Extracell. Vesicles* 2014, 3, 23262.
- [20] Sodar, B. W., Kittel, A., Paloczi, K., Vukman, K. V., Osteikoetxea, X., Szabo-Taylor, K., Nemeth, A., Sperlagh, B., Baranyai, T., Giricz, Z., Wiener, Z., Turiak, L., Drahos, L., Pallinger, E., Vekey, K., Ferdinandy, P., Falus, A., Buzas, E. I., *Sci. Rep.* 2016, 6, 24316.
- [21] Welton, J. L., Webber, J. P., Botos, L. A., Jones, M., Clayton, A., *J. Extracell. Vesicles* 2015, 4, 27269.
- [22] de Menezes-Neto, A., Saez, M. J., Lozano-Ramos, I., Segui-Barber, J., Martin-Jaular, L., Ullate, J. M., Fernandez-Becerra, C., Borrás, F. E., Del Portillo, H. A., *J. Extracell. Vesicles* 2015, 4, 27378.
- [23] Cao, F., Gao, Y., Chu, Q., Wu, Q., Zhao, L., Lan, T., Zhao, L., *Electrophoresis* 2019, 40, 3092–3098.
- [24] Rider, M. A., Hurwitz, S. N., Meckes, D. G., Jr., *Sci. Rep.* 2016, 6, 23978.
- [25] Yang, F., Liao, X., Tian, Y., Li, G., *Biotechnol. J.* 2017, 12, 1600699.
- [26] Wu, M., Ouyang, Y., Wang, Z., Zhang, R., Huang, P. H., Chen, C., Li, H., Li, P., Quinn, D., Dao, M., Suresh, S., Sadovsky, Y., Huang, T. J., *Proc. Natl. Acad. Sci. U. S. A.* 2017, 114, 10584–10589.
- [27] Liu, C., Guo, J., Tian, F., Yang, N., Yan, F., Ding, Y., Wei, J., Hu, G., Nie, G., Sun, J., *ACS Nano* 2017, 11, 6968–6976.
- [28] Zhao, Z., Yang, Y., Zeng, Y., He, M., *Lab Chip* 2016, 16, 489–496.
- [29] Lewis, J. M., Vyas, A. D., Qiu, Y., Messer, K. S., White, R., Heller, M. J., *ACS Nano* 2018, 12, 3311–3320.
- [30] Li, P., Kaslan, M., Lee, S. H., Yao, J., Gao, Z., *Theranostics* 2017, 7, 789–804.
- [31] Bruce, T. F., Slonecki, T. J., Wang, L., Huang, S., Powell, R. R., Marcus, R. K., *Electrophoresis* 2019, 40, 571–581.
- [32] Huang, S., Wang, L., Bruce, T. F., Marcus, R. K., *Anal. Bioanal. Chem.* 2019, 411, 6591–6601.
- [33] Wang, L., Bruce, T. F., Huang, S., Marcus, R. K., *Anal. Chim. Acta* 2019, 1082, 186–193.
- [34] Huang, S., Wang, L., Bruce, T. F., Marcus, R. K., *Biotechnol. Prog.* 2020, e2998.
- [35] Jackson, K. K., Powell, R. R., Bruce, T. F., Marcus, R. K., *Anal. Bioanal. Chem.* 2020, 412, 4713–4724.
- [36] Randunu, K. M., Marcus, R. K., *Anal. Bioanal. Chem.* 2012, 404, 721–729.

- [37] Vergauwen, G., Dhondt, B., Van Deun, J., De Smedt, E., Berx, G., Timmerman, E., Gevaert, K., Miinalainen, I., Cocquyt, V., Braems, G., Van den Broecke, R., Denys, H., De Wever, O., Hendrix, A., *Sci. Rep.* 2017, 7, 2704.
- [38] Wisniewski, J. R., *Methods Mol. Biol.* 2018, 1841, 3–10.
- [39] An, M., Zou, X., Wang, Q., Zhao, X., Wu, J., Xu, L. M., Shen, H. Y., Xiao, X., He, D., Ji, J., *Anal. Chem.* 2013, 85, 4530–4537.
- [40] Cox, J., Mann, M., *Nat. Biotechnol.* 2008, 26, 1367–1372.
- [41] Pathan, M., Keerthikumar, S., Chisanga, D., Alessandro, R., Ang, C. S., Askenase, P., Batagov, A. O., Benito-Martin, A., Camussi, G., Clayton, A., Collino, F., Di Vizio, D., Falcon-Perez, J. M., Fonseca, P., Fonseka, P., Fontana, S., Gho, Y. S., Hendrix, A., Hoen, E. N., Iraci, N., Kastaniegaard, K., Kislinger, T., Kowal, J., Kurochkin, I. V., Leonardi, T., Liang, Y., Llorente, A., Lunavat, T. R., Maji, S., Monteleone, F., Øverbye, A., Panaretakis, T., Patel, T., Peinado, H., Pluchino, S., Principe, S., Ronquist, G., Royo, F., Sahoo, S., Spinelli, C., Stensballe, A., Théry, C., van Herwijnen, M. J. C., Wauben, M., Welton, J. L., Zhao, K., Mathivanan, S., *J. Extracell. Vesicles* 2017, 6, 1321455.
- [42] The Gene Ontology Consortium, *Nucleic Acids Res.* 2015, 43, D1049–D1056.
- [43] Pathan, M., Fonseka, P., Chitti, S. V., Kang, T., Sanwlani, R., Van Deun, J., Hendrix, A., Mathivanan, S., *Nucleic Acids Res.* 2019, 47, D516–D519.
- [44] Thery, C., Witwer, K. W., Aikawa, E., Alcaraz, M. J., Anderson, J. D., Andriantsitohaina, R., Antoniou, A., Arab, T., Archer, F., Atkin-Smith, G. K., Ayre, D. C., Bach, J.-M., Bachurski, D., Baharvand, H., Balaj, L., Baldacchino, S., Bauer, N. N., Baxter, A. A., Bebawy, M., Beckham, C., Bedina Zavec, A., Benmoussa, A., Berardi, A. C., Bergese, P., Bielska, E., Blenkiron, C., Bobis-Wozowicz, S., Boilard, E., Boireau, W., Bongiovanni, A., Borràs, FE., Bosch, S., Boulanger, C. M., Breakefield, X., Breglio, A. M., Brennan, M. Á., Brigstock, D. R., Brisson, A., Broekman, M. L. D., Bromberg, J. F., Bryl-Górecka, P., Buch, S., Buck, A. H., Burger, D., Busatto, S., Buschmann, D., Bussolati, B., Buzás, E. I., Byrd, J. B., Camussi, G., Carter, D. R. F., Caruso, S., Chamley, L. W., Chang, Y. T., Chen, C., Chen, S., Cheng, L., Chin, A. R., Clayton, A., Clerici, S. P., Cocks, A., Cocucci, E., Coffey, R. J., Cordeiro-da-Silva, A., Couch, Y., Coumans, F. A. W., Coyle, B., Crescitelli, R., Criado, M. F., D'Souza-Schorey, C., Das, S., Datta, Chaudhuri, A., de Candia, P., De Santana, E. F., De Wever, O., Del Portillo, H. A., Demaret, T., Deville, S., Devitt, A., Dhondt, B., Di Vizio, D., Dieterich, L. C., Dolo, V., Dominguez Rubio, A. P., Dominici, M., Dourado, M. R., Driedonks, T. A. P., Duarte, F. V., Duncan, H. M., Eichenberger, R. M., Ekström, K., El Andaloussi, S., Elie-Caille, C., Erdbrügger, U., Falcón-Pérez, J. M., Fatima, F., Fish, J. E., Flores-Bellver, M., Försonits, A., Frelet-Barrand, A., Fricke, F., Fuhrmann, G., Gabrielsson, S., Gámez-Valero, A., Gardiner, C., Gärtner, K., Gaudin, R., Gho, Y. S., Giebel, B., Gilbert, C., Gimona, M., Giusti, I., Goberdhan, D. C. I., Görgens, A., Gorski, S. M., Greening, D. W., Gross, J. C., Gualerzi, A., Gupta, G. N., Gustafson, D., Handberg, A., Haraszti, R. A., Harrison, P., Hegyesi, H., Hendrix, A., Hill, A. F., Hochberg, F. H., Hoffmann, K. F., Holder, B., Holthofer, H., Hosseinkhani, B., Hu, G., Huang, Y., Huber, V., Hunt, S., Ibrahim, A. G.-E., Ikezu, T., Inal, J. M., Isin, M., Ivanova, A., Jackson, H. K.,

Jacobsen, S., Jay, S. M., Jayachandran, M., Jenster, G., Jiang, L., Johnson, S. M., Jones, J. C., Jong, A., Jovanovic-Taliman, T., Jung, S., Kalluri, R., Kano, SI., Kaur, S., Kawamura, Y., Keller, E. T., Khamari, D., Khomyakova, E., Khvorova, A., Kierulf, P., Kim, K. P., Kislinger, T., Klingeborn, M., Klinke, D. J., 2nd., Kornek, M., Kosanović, M. M., Kovács, Á. F., Krämer-Albers, E.-M., Krasemann, S., Krause, M., Kurochkin, I. V., Kusuma, G. D., Kuypers, S., Laitinen, S., Langevin, S. M., Languino, L. R., Lannigan, J., Lässer, C., Laurent, L. C., Lavieu, G., Lázaro-Ibáñez, E., Le Lay, S., Lee, M.-S., Lee, Y. X. F., Lemos, D. S., Lenassi, M., Leszczynska, A., Li, I. T., Liao, K., Libregts, S. F., Ligeti, E., Lim, R., Lim, S. K., Linē, A., Linnemannstöns, K., Llorente, A., Lombard, C. A., Lorenowicz, M. J., Lőrincz, Á. M., Lötval, J., Lovett, J., Lowry, M. C., Loyer, X., Lu, Q., Lukomska, B., Lunavat, T. R., Maas, S. L. N., Malhi, H., Marcilla, A., Mariani, J., Mariscal, J., Martens-Uzunova, E. S., Martin-Jaular, L., Martinez, M. C., Martins, V. R., Mathieu, M., Mathivanan, S., Maugeri, M., McGinnis, L. K., McVey, M. J., Meckes, D. G., Jr., Meehan, K. L., Mertens, I., Minciacchi, V. R., Möller, A., Møller Jørgensen, M., Morales-Kastresana, A., Morhayim, J., Mullier, F., Muraca, M., Musante, L., Mussack, V., Muth, D. C., Myburgh, K. H., Najrana, T., Nawaz, M., Nazarenko, I., Nejsun, P., Neri, C., Neri, T., Nieuwland, R., Nimrichter, L., Nolan, J. P., Nolte-'t, Hoen, E. N. M., Noren, Hooten, N., O'Driscoll, L., O'Grady, T., O'Loughlen, A., Ochiya, T., Olivier, M., Ortiz, A., Ortiz, L. A., Osteikoetxea, X., Østergaard, O., Ostrowski, M., Park, J., Pegtel, D. M., Peinado, H., Perut, F., Pfaffl, M. W., Phinney, D. G., Pieters, B. C. H., Pink, R. C., Pisetsky, D. S., Pogge, von Strandmann, E., Polakovicova, I., Poon, I. K. H., Powell, B. H., Prada, I., Pulliam, L., Quesenberry, P., Radeghieri, A., Raffai, R. L., Raimondo, S., Rak, J., Ramirez, M. I., Raposo, G., Rayyan, M. S., Regev-Rudzki, N., Ricklefs, F. L., Robbins, P. D., Roberts, D. D., Rodrigues, S. C., Rohde, E., Rome, S., Rouschop, K. M. A., Rughetti, A., Russell, A. E., Saá, P., Sahoo, S., Salas-Huenuleo, E., Sánchez, C., Saugstad, J. A., Saul, M. J., Schiffelers, R. M., Schneider, R., Schøyen, T. H., Scott, A., Shahaj, E., Sharma, S., Shatnyeva, O., Shekari, F., Shelke, G. V., Shetty, A. K., Shiba, K., Siljander, P. R.-M., Silva, A. M., Skowronek, A., Snyder, O. L., 2nd., Soares, R. P., Sódar, B. W., Soekmadji, C., Sotillo, J., Stahl, P. D., Stoorvogel, W., Stott, S. L., Strasser, E. F., Swift, S., Tahara, H., Tewari, M., Timms, K., Tiwari, S., Tixeira, R., Tkach, M., Toh, W. S., Tomasini, R., Torrecilhas, A. C., Tosar, J. P., Toxavidis, V., Urbanelli, L., Vader, P., van Balkom, B. W. M., van der Grein, S. G., Van Deun, J., van Herwijnen, M. J. C., Van Keuren-Jensen, K., van Niel, G., van Royen, M. E., van Wijnen, A. J., Vasconcelos, M. H., Vechetti, I. J., Jr., Veit, T. D., Vella, L. J., Velot, É., Verweij, F. J., Vestad, B., Viñas, J. L., Visnovitz, T., Vukman, K. V., Wahlgren, J., Watson, D. C., Wauben, M. H. M., Weaver, A., Webber, J. P., Weber, V., Wehman, A. M., Weiss, D. J., Welsh, J. A., Wendt, S., Wheelock, A. M., Wiener, Z., Witte, L., Wolfram, J., Xagorari, A., Xander, P., Xu, J., Yan, X., Yáñez-Mó, M., Yin, H., Yuana, Y., Zappulli, V., Zarubova, J., Žekas, V., Zhang, J.-y., Zhao, Z., Zheng, L., Zheutlin, A. R., Zickler, A. M., Zimmermann, P., Zivkovic, A. M., Zocco, D., Zuba-Surma, E. K., *J. Extracell. Vesicles* 2018, 7, 1535750.

- [45] Tauro, B. J., Greening, D. W., Mathias, R. A., Ji, H., Mathivanan, S., Scott, A. M., Simpson, R. J., *Methods* 2012, *56*, 293–304.
- [46] Piersma, S. R., Fiedler, U., Span, S., Lingnau, A., Pham, T. V., Hoffmann, S., Kubbutat, M. H., Jiménez, C. R., *J. Proteome Res.* 2010, *9*, 1913–1922.
- [47] Anderson, N. L., Anderson, N. G., *Mol. Cell. Proteomics* 2002, *1*, 845–867.
- [48] Tirumalai, R. S., Chan, K. C., Prieto, D. A., Issaq, H. J., Conrads, T. P., Veenstra, T. D., *Mol. Cell. Proteomics* 2003, *2*, 1096–1103.
- [49] An, M., Wu, J., Zhu, J., Lubman, D. M., *J. Proteome Res.* 2018, *17*, 3599–3605.
- [50] Worsfold, P., Townshend, A., Poole, C. F., Miró, M., *Encyclopedia of Analytical Science, 3rd Edition*, Elsevier, Amsterdam 2019.
- [51] Chen, Y., Xie, Y., Xu, L., Zhan, S., Xiao, Y., Gao, Y., Wu, B., Ge, W., *Int. J. Cancer* 2017, *140*, 900–913.
- [52] Brennan, K., Martin, K., FitzGerald, S. P., O'Sullivan, J., Wu, Y., Blanco, A., Richardson, C., Mc Gee, M. M., *Sci. Rep.* 2020, *10*, 1039.

Figure captions

Figure 1. Workflow of EV separation from microliter-scale of human serum using PET C-CP HIC method followed by a post-column cleanup protocol with different RC-CFs (regenerated cellulose centrifugal filters; MWCO 10kDa/100kDa) for down-stream EV characterization and EV proteome profiling, respectively.

Figure 2. (A) Chromatograms of EV separation from 20 μ L of human serum with different elution times with the second step gradient, 50% glycerol, starting at 6, 8, 10, 12 and 14 min, respectively. **(B)** SDS-PAGE analysis followed by silver staining. Two separate images: Left, protein ladder and 0.05 μ g of BSA, respectively; Right, EV fractions derived from 40 μ L of serum with the second step gradient starting at 6 and 14 min, respectively.

Figure 3. Comparative analysis of different MWCO centrifugal filters, 10kD/50kD/100kD, for EV sample concentration and further purification. **(A)** Particle recovery was analyzed using Nanoparticle tracking analysis ($n = 5$, $**p < 0.01$, $***p < 0.001$). Data are expressed as mean \pm SD. **(B)** SDS-PAGE analysis coupled with silver staining. Two separate images: Left, protein ladder as an indicator of protein molecular weight; Right, the concentrated EV samples using different MWCO centrifugal filters, with BSA as a reference.

Figure 4. EV characterization. **(A)** TEM image of the eluted EVs after post-cleaning (scale = 200 nm); the insert shows EVs with higher magnification. **(B)** NTA measurement of the size distribution of eluted EVs after post-cleaning. **(C)** Western blotting image of EV markers (CD63 and CD9).

Figure 5. Bioinformatics Analysis. **(A)** Venn diagram showing the overlap of proteins identified in this study versus the Vesiclepedia database. **(B-D)** Gene Ontology analysis showing the six most enriched categories and the enrichment significance ($-\log(p\text{-value})$, $p < 0.05$) of the identified proteins in cellular components **(B)**, biological process **(C)**, and molecular functions **(D)**.

Figure 6. Comparison of the major contaminating proteins, i.e., the top 10 blood proteins and apolipoproteins, in serum-derived EVs isolated by the PET C-CP HIC method versus other separation methods (UC, SEC, and precipitation). **(A)** Comparison with previous study in our laboratory (“n” indicates sample size). Optimized UC*: 100 000 g for 120 min + 100 000 g for 70 min \times 4 cycles. UC*: 100 000 g for 120 min. **(B)** Comparison with other studies (“n” indicates sample size). UC*: 110 000 g for 90 min.

Figure 1

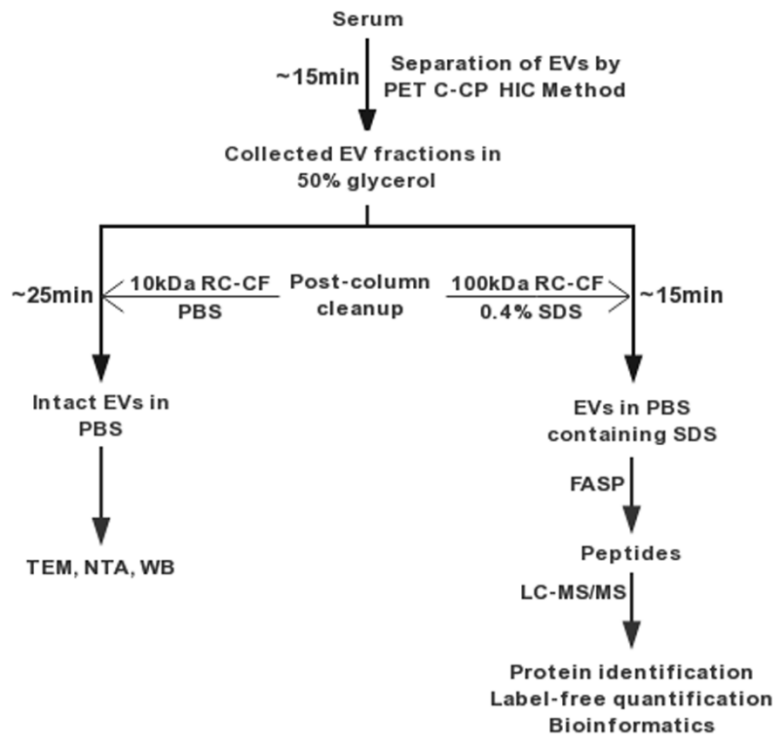


Figure 2

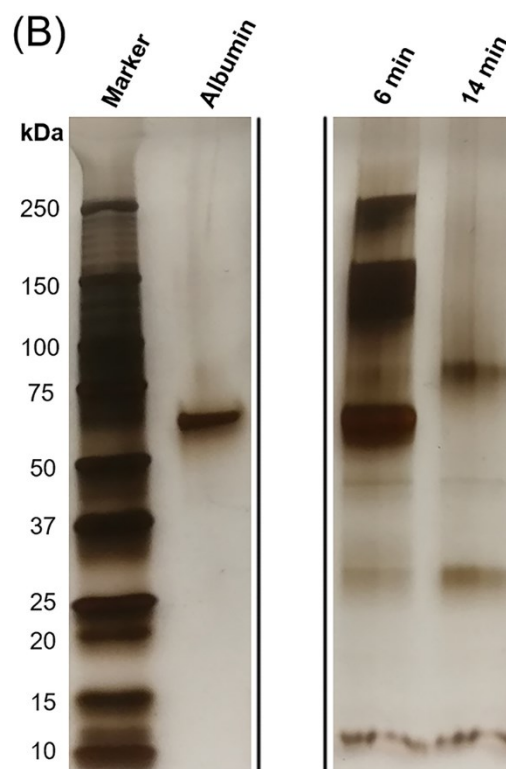
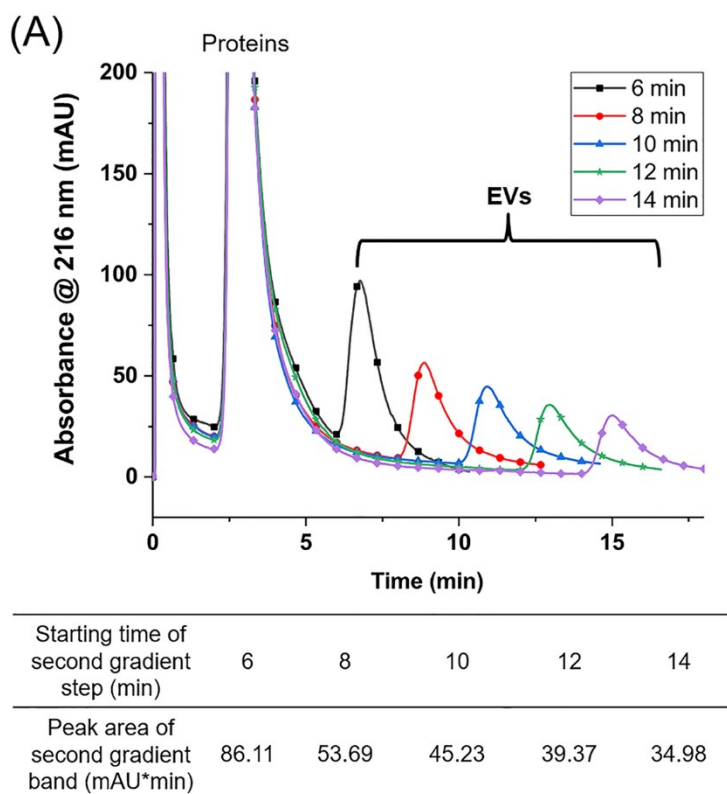


Figure 3

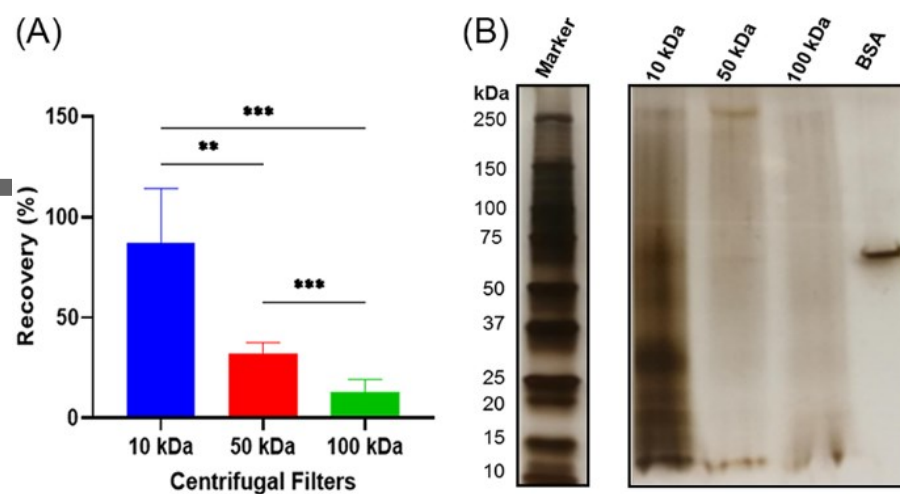


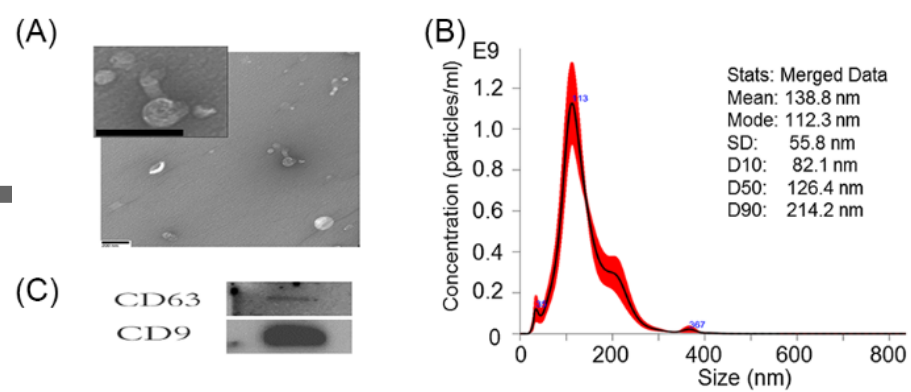
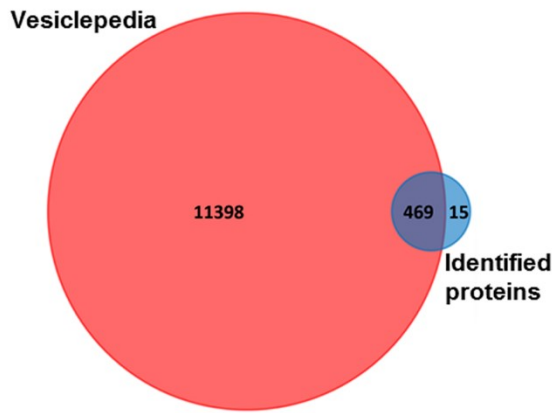
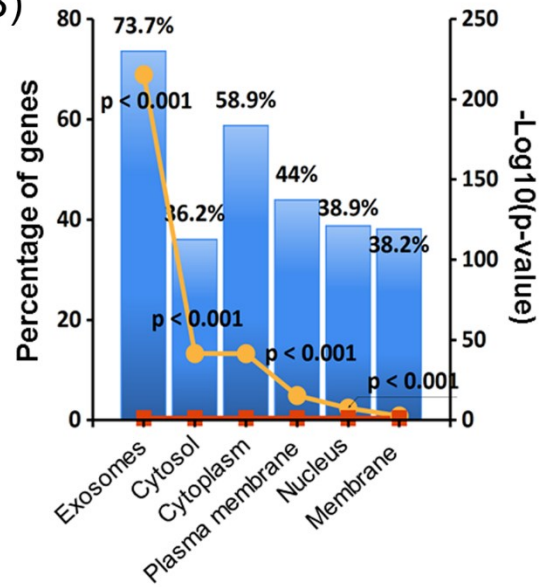
Figure 4

Figure 5

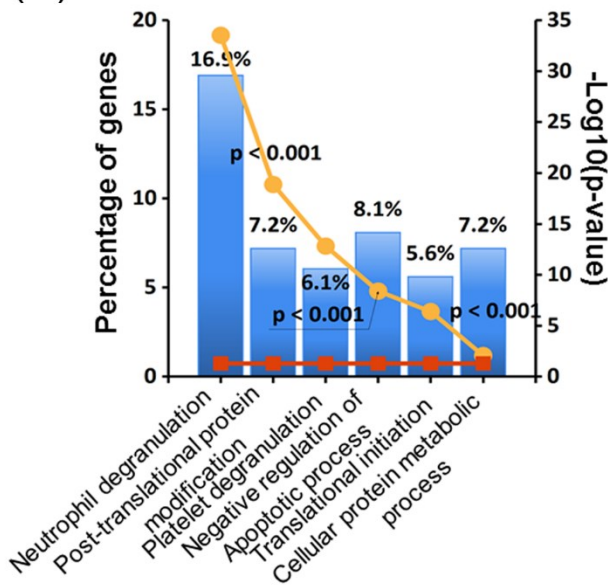
(A)



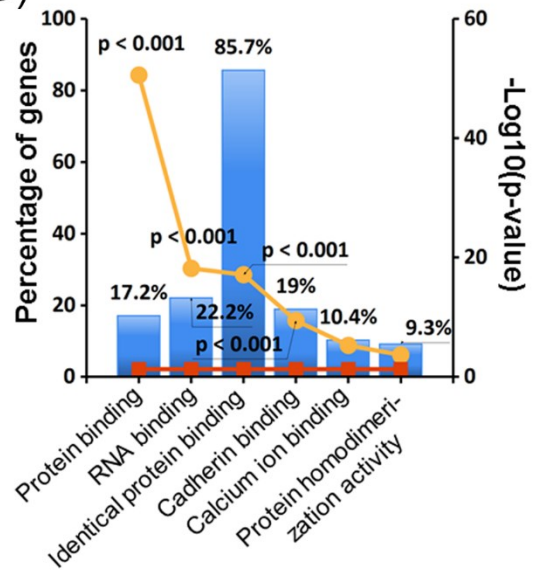
(B)



(C)



(D)



Author Manuscript

Figure 6

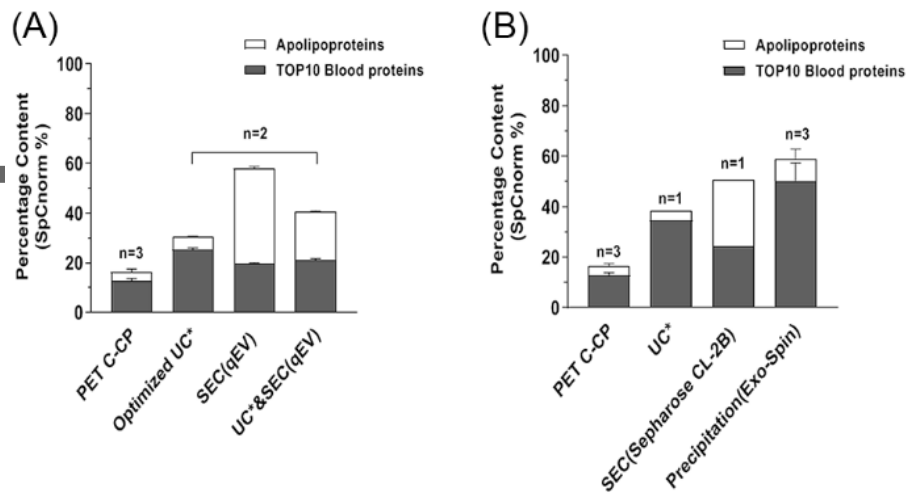
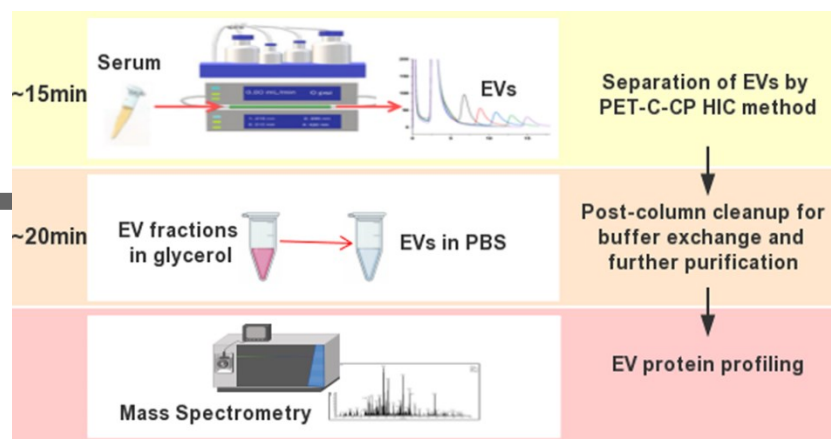


Table 1. EV markers identified in this study

Category	Human Gene Name
Transmembrane or GPI-anchored proteins	1a) Non-tissue specific CD63, CD81, CD82, HLA-A, H2-K/D/Q, ITGA2/3/6/V, ITGB1/3/4, LAMP1, NT5E, CD55, CD59
	1b) Cell/tissue specific TSPAN8, ERBB2, EPCAM, CD14, ABCC1
Cytosolic proteins recovered in EVs	2a) With lipid or membrane protein-binding ability CHMP1B/4B, PDCD6IP, FLOT1/2, EHD4, ANXA1/2/4/5/7/11/13, HSPA8, HSP90AB1, SDCBP2
	2b) Promiscuous incorporation in EVs (and possibly exomeres) HSPA1A, ACTB, TUBA/B, GAPDH
Others	HIST1H4A, LMNA, HSP90B1, HSPA5, ACTN4, FN1, LGALS3BP, CD5L, AHSG

For TOC only



Author Manuscript